



Protocol using wide-detector CT with single contrast injection for the aorta and coronary artery: variable helical pitch versus volume scan following helical scan

Nari Shin¹ · Sung Mok Kim² · Yeon Hyeon Choe²

Received: 3 March 2019 / Accepted: 27 May 2019 / Published online: 6 June 2019
© Springer Nature B.V. 2019

Abstract

The aim of this study was to compare the radiation dose and image quality of two CT protocols using a wide-detector computed tomography (WDCT) scanner with single contrast injection for simultaneous evaluation of the aorta and coronary artery. We retrospectively included 104 consecutive patients who underwent coronary and aorta CT angiography. CT Protocols were divided as follows: protocol I, variable helical pitch scan (VHP, n = 31); protocol II, volume scan for coronary artery following helical scan for aorta (VFH, n = 73). Vascular attenuation, noise, signal-to-noise (SNR), and contrast-to-noise ratios (CNR) were compared. Image parameters were measured at coronary artery, thoracic aorta, abdominal aorta, and iliofemoral arteries. Subjective image quality was assessed by two observers. The patient characteristics between groups were similar ($P \geq 0.384$). There were no significant differences in any of the quantitative image parameters between the two groups except for the thoracic aorta. Vascular attenuation (469.2 ± 133.6 vs. 605.9 ± 140.2 HU), CNR (24.8 ± 11.4 vs. 37.3 ± 18.5), and SNR (28.4 ± 12.0 vs. 40.6 ± 19.5 ml) were higher in the VHP protocol ($P < 0.001$ for each) for covering the thoracic aorta. However, all subjective image scores guaranteed diagnostic image quality. The effective radiation dose of the VFH protocol was reduced to 27.2% compared with that of the VHP protocol (443.8 ± 115.8 vs. 706.7 ± 163.7 mGy-cm, $P < 0.001$). WDCT with single contrast injection allows assessment of both the coronary artery and aorta. The VFH protocol can reduce the radiation dose and preserve the image quality compared with that of the VHP protocol.

Keywords Wide-detector computed tomography · Aorta · Coronary vessels · Image quality · Radiation dose

Abbreviations

BMI	Body mass index
CAD	Coronary artery disease
CCTA	Coronary CT angiography
CNR	Contrast-to-noise ratio
ECG	Electrocardiogram
HU	Hounsfield unit
MDCT	Multidetector computed tomography
NI	Noise index
SNR	Signal-to-noise ratio

TAVI	Transcatheter aortic valve implantation
VFH	Volume following helical
VHP	Variable helical pitch
WDCT	Wide detector computed tomography

Introduction

Coronary CT angiography (CCTA) has become a very useful technique for depiction of coronary artery disease (CAD). In addition to providing dedicated imaging for coronary artery diseases, ECG gating is required for diagnosis of aortic disease and for pre-procedural planning and post-intervention evaluation. Patients with thoracoabdominal aortic aneurysm often have severe ischemic heart disease. In such cases, simultaneous operations on both the aorta and the heart may be necessary [1, 2]. In patients with aortic dissection, coronary malperfusion due to concomitant coronary dissection is a relatively rare but fatal condition [3, 4]. Previous study reported the incidence of coronary malperfusion associated

✉ Sung Mok Kim
sungmok_kim@hanmail.net

¹ Department of Radiology, Samsung Medical Center, Sungkyunkwan University School of Medicine, Seoul, Republic of Korea

² Department of Radiology and Cardiovascular Imaging Center, Heart Vascular Stroke Institute, Samsung Medical Center, Sungkyunkwan University School of Medicine, 81 Ilwon-ro, Gangnam-gu, Seoul 06351, Republic of Korea

with acute type A aortic dissection to be 6.1% and described the causes of malperfusion as follows: coronary artery occlusion resulting from compression by the bulging dissected false lumen, retrograde extension of the dissection into the coronary arterial wall, detached coronary artery from the aortic root [5]. In Takayasu arteritis, coronary involvement is not rare, as it is detected in approximately 44–54% of cases at CCTA [6, 7]. In pre-procedural planning for transcatheter aortic valve implantation (TAVI), both aortic root anatomy and feasibility of valve delivery through the femoral arteries or other access routes must be determined prior to the implantation procedure [8–10]. In these patients, simultaneous examinations of the aorta and coronary arteries are helpful in determining the treatment plan.

The development wide-detector CT (WDCT) can acquire the cardiac volume in a single heartbeat and it has a number of significant advantages. Firstly, misregistration artefacts are completely avoided, particularly in patients with irregular heart rates. Secondly, the volume of the contrast agent can be reduced and thirdly, the scanners are ideally suited to performing dynamic myocardial perfusion studies [11]. Recently, the next-generation WDCT enables variable helical pitch (VHP) scanning using two pitch changes and volume following helical (VFH) scanning. These scan techniques have led to simultaneous image acquisition of the aorta and heart during single contrast injection. Previous studies have demonstrated the feasibility of VHP scanning for TAVI [12]. However, the study used VHP with only one pitch change and did not introduce VFH scanning. The aim of the current study

was to compare the radiation dose and image quality of two CT protocols using a WDCT scanner with single contrast injection for simultaneous evaluation of the aorta and coronary artery.

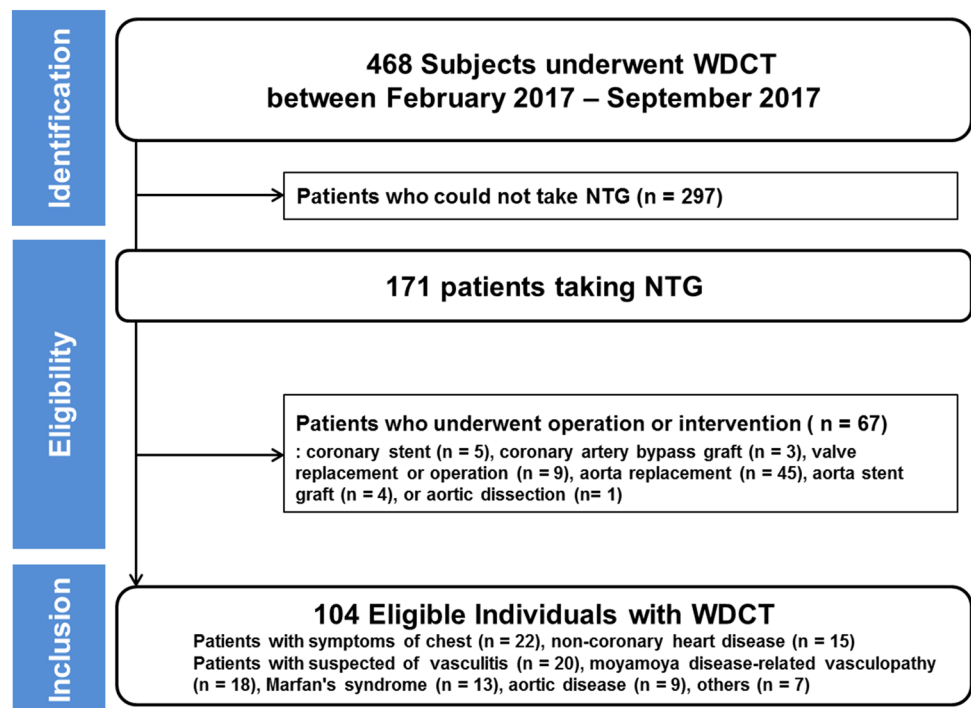
Methods

This retrospective image analysis study was approved by our institutional review board, and written informed consent was waived.

Subjects

The study was based on the CT data of 468 subsequent patients who underwent a CT exam for simultaneous assessment of the heart and aorta using a WDCT between February 2017 and September 2017. For accurate image assessment, we excluded patients who could not take nitroglycerin. From the remaining patients ($n = 171$), we excluded those who underwent operation or interventional procedure before CT scan (Fig. 1). Ultimately, 104 patients were included in our analysis and their major findings of CT examination were as follows: normal ($n = 45$), minimal CAD ($n = 11$), mild CAD ($n = 19$), moderate CAD ($n = 5$), vasculitis of aorta or neck vessels ($n = 14$), annuloaortic ectasia ($n = 6$), dissection or stenosis of superior mesenteric artery ($n = 4$).

Fig. 1 Flow chart of enrollment



CT protocol

All patients underwent electrocardiogram (ECG)-gated and contrast-enhanced CT using a WDCT system (Aquilion ONE/Genesis Edition, Canon Medical Systems, Otawara, Japan). Patients with a pre-scan heart rate of 65 bpm or higher were given 50–100 mg of oral metoprolol 60 min prior to the CT examination, unless the subject had a contraindication to beta-blockers. After scanning for calcium scoring, 0.4 mg of sublingual nitroglycerin was administered to all patients without contraindication.

CT examinations were performed using the following parameters: peak tube voltage, 100 kV; tube current, 100–400 mA for thoracoabdominal area and 40–400 mA for cardiac area; (determined based on a pre-specified BMI protocol); rotation speed, 0.275 s; and slice collimation, 0.5×100 mm; and iterative reconstruction mode (AIDR3D, standard mode, Canon Medical Systems). This WDCT equipment allows a seamless change in the scan pitch during one continuous acquisition and enables a combination of gated and non-gated acquisitions within one scan. A pitch of 0.15–0.17 was chosen for ECG-gated cardiac imaging depending on the patient's heart rate, and 0.87 was used for non-ECG-gated aorta scan.

In VHP scanning (Fig. 2a), non-ECG-gated scanning of the upper chest was started from approximately 2 cm above the lung apex to the carina. Then, retrospective ECG-gated scanning began from the carina to the base

of the heart. For the abdominal aorta and iliac arteries, non-ECG-gated scanning was used. The retrospective ECG-gated helical scan was used with the full radiation dose window set at 65% to 80% of the R-R interval in patients with heart rate ≤ 70 bpm and at 30% to 50% in patients with a heart rate > 70 bpm. A reduced dose (20% of the dose during the acquisition window) was used for the remainder of the R-R interval to minimize the radiation dose.

In VFH scanning (Fig. 2b), a prospective ECG-triggering axial scan was used to cover heart, and non-ECG-gated scanning was then used for the aorta and iliac arteries. The field of view of the maximal 16 cm in the z-axis, covered by the 320 detector rows of 0.5 mm each, allowed axial volumetric scanning of the heart without table movement. After ECG-triggering axial scanning of the heart, the table moved for the aorta scanning from approximately 2 cm above the lung apex to the iliac arteries. The prospective ECG-triggering axial scan was used with the full radiation dose window set at 65% to 80% of the R-R interval in patients with heart rate ≤ 70 bpm and at 30% to 50% in patients with a heart rate > 70 bpm.

A nonionic contrast medium (Iomeron 400; Bracco Diagnostics, Milan, Italy) was injected into the antecubital vein at 4–5 mL/s, followed by 30–40 mL of normal saline at the same flow rate. The CT acquisition delay time was calculated as the time of peak contrast medium attenuation in a region of interest in the ascending aorta plus 3 s.

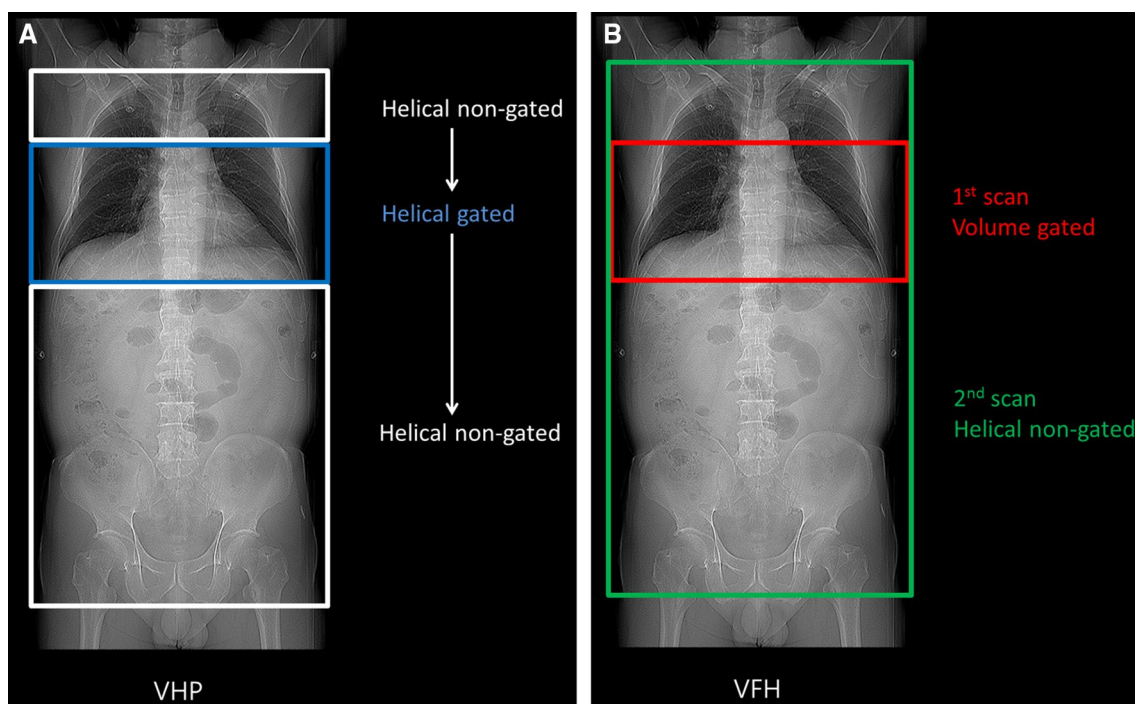


Fig. 2 a Variable helical pitch scan protocol (VHP) b Volume following helical scan protocol (VFH)

Quantitative image assessment

Quantitative analysis of the CT images was performed by two independent, blinded radiologists who analyzed 2.0 mm thick transverse images for aorta and 0.5 mm thick transverse images for coronary vessel. The aorta and iliofemoral attenuation values were measured in ROIs as follows: aortic root, ascending thoracic aorta, descending thoracic aorta (at the level of the pulmonary artery bifurcation), abdominal aorta (at each level of renal artery ostium and just above iliac bifurcation), both common iliac arteries, both external iliac arteries, and both common femoral arteries (Fig. 3). The muscle attenuation values were measured within the ROI in the subscapularis muscle (for thoracic aorta), bilateral paraspinal muscle (for the abdominal aorta), and gluteus muscle (for iliofemoral artery). The coronary artery attenuation values were measured in ROIs in the left main, proximal left anterior descending, proximal left circumflex, and proximal right coronary artery. Additional ROI measurements were performed in the adjacent pericardial fat.

ROIs were scaled as large as possible while excluding the vascular wall, vascular calcification or non-calcified plaque, and artifacts. Intravascular attenuation was measured in Hounsfield unit (HU), and vessel noise was defined as the standard deviation of all ROI measurements. The image noise was defined as the standard deviation of the CT attenuation values of the muscle and pericardial fat. A total of three ROI measurements was repeated at each location and averaged to ensure data consistency. The mean attenuation values of the whole aorta, coronary vessels, muscles,

and pericardial fat were calculated by averaging the values obtained from two observers.

The signal-to-noise ratio (SNR) and contrast-to-noise ratio (CNR) were calculated using the following formulas: for aortic assessment, $SNRa = \text{mean aortic attenuation} / \text{image noise}$, $CNRa = (\text{mean aortic attenuation} - \text{muscle attenuation}) / \text{image noise}$; for coronary assessment, $SNRc = \text{mean coronary attenuation} / \text{image noise}$, $CNRc = (\text{mean coronary attenuation} - \text{perivascular fat attenuation}) / \text{image noise}$.

Qualitative image assessment

Subjective image quality (IQ) of vascular contrast attenuation and image noise were assessed for the cardiac and the aortoiliac image series independently by two experienced observers. In discordant scores, consensus reading was then performed between two observers who evaluated subjective IQ.

The IQ values of attenuation for the coronary and the aortoiliac vasculatures were assessed with a 5-point Likert scale as follows: score of 1, insufficient attenuation resulting in a non-diagnostic examination; 2, poor, suboptimal attenuation with low diagnostic confidence; 3, fair, acceptable attenuation of relevant cardiac anatomy and vascular access; 4, good, satisfactory attenuation providing sufficient evaluation of relevant anatomy; 5, excellent, strong attenuation of even the smallest arteries [13].

The presence and extent of image artifact were assessed with a 5-point Likert scale as follows: score of 1,

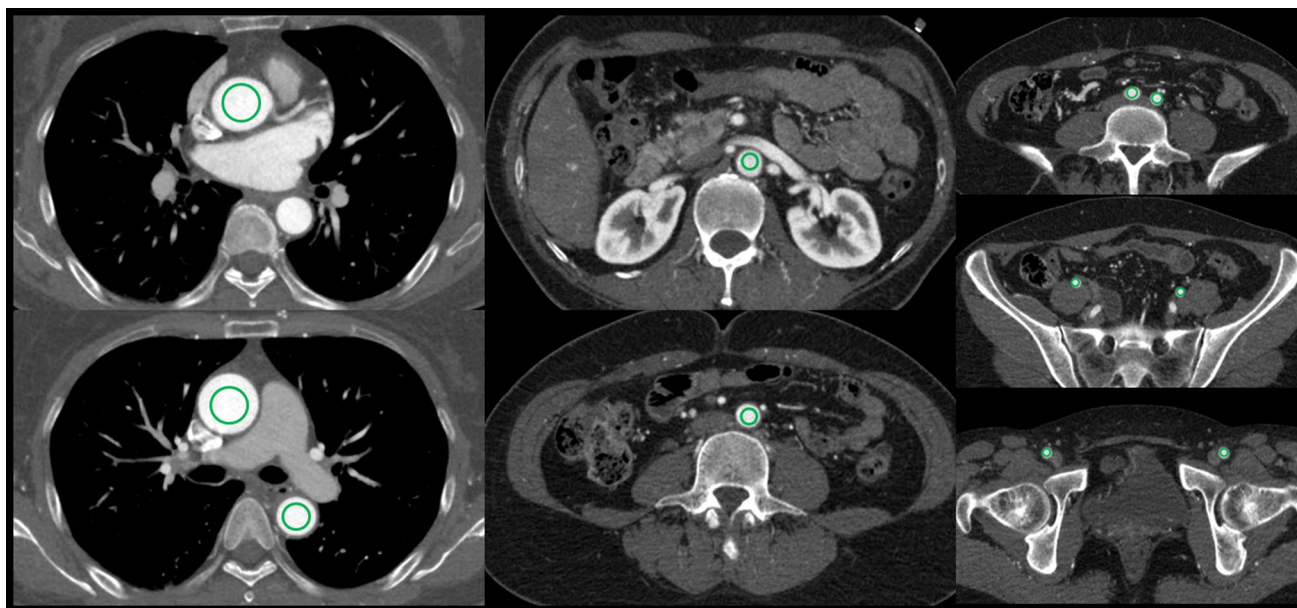


Fig. 3 The aorta and iliofemoral attenuation values were measured using ROIs in the aortic root, ascending thoracic aorta, descending thoracic aorta, abdominal aorta, both common iliac arteries, both external iliac arteries, and both common femoral arteries

non-diagnostic, severe artifact; 2, poor, substantial artifact but sufficient contrast attenuation for assessing cardiovascular anatomy; 3, fair, moderate artifact not interfering with a comprehensive examination of the heart and vascular system; 4, good, with only minor artifact not interfering with assessment; 5, excellent, with no artifact or any diagnostic limitation [13].

Radiation exposure

The effective radiation dose for each component of the CT examination was calculated as the product of the dose-length product multiplied by a conversion coefficient ($k=0.014 \text{ mSv}/[\text{mGycm}]$) [14].

Statistical analysis

All continuous variables are expressed as mean \pm standard deviation, whereas categorical data are expressed as frequency and percentage. The *t* test was used for normally distributed data, whereas Wilcoxon signed rank test was used for data that were not normally distributed in continuous variables. Fisher's exact test was used to evaluate the significance of differences in categorical variables between groups. Interobserver agreement for the measurement of image quality was analyzed with intraclass correlation coefficients (ICCs). ICC values of 0.20 or less were indicative of poor agreement; 0.21–0.40 was considered fair; 0.41–0.60, moderate; 0.61–0.80, good; and 0.81 or more, excellent correlation. In all statistical analyses, *p* values < 0.05 were considered statistically significant.

Results

Patient characteristics

Patient characteristics are listed in Table 1. There were no significant differences in age, sex, heart rate, or BMI between the two groups of patients. Contrast volume (61.0 ± 7.5 vs. 72.9 ± 5.1 ml) and saline volume (30.7 ± 4.2 vs. 44.2 ± 9.2 ml) were significantly lower with VFH than VHP ($P < 0.001$).

Quantitative image quality

At cardiac, abdominal aorta, and iliofemoral levels, there were no statistically significant differences in vessel attenuation, vessel noise, image noise, SNR, and CNR between VFH and VHP protocols (all $P_s \geq 0.104$). In the assessment of the thoracic aorta, the vessel attenuation (469.2 ± 133.6

Table 1 Patient characteristics

	VHP	VFH	P value
n	31	73	
Age (years)	48.7 ± 17.2	51.4 ± 15.4	0.429
Sex (male, n)	15	39	0.384
Height (cm)	167.0 ± 9.0	165.9 ± 8.9	0.576
Weight (kg)	67.2 ± 12.1	66.1 ± 11.1	0.653
Heart rate (bpm)	65.2 ± 8.9	64.3 ± 14.7	0.165
Body mass index (kg/m^2)	24.7 ± 3.76	23.9 ± 3.0	0.398
BSA (m^2)	1.8 ± 0.2	1.8 ± 0.2	0.624
Contrast volume (ml)	72.9 ± 5.1	61.0 ± 7.5	< 0.001
Contrast flow (ml/sec)	4.5 ± 0.5	4.7 ± 0.4	0.012
Saline volume (ml)	44.2 ± 9.2	30.7 ± 4.2	< 0.001
Saline flow (ml/sec)	4.5 ± 0.5	4.7 ± 0.4	0.012

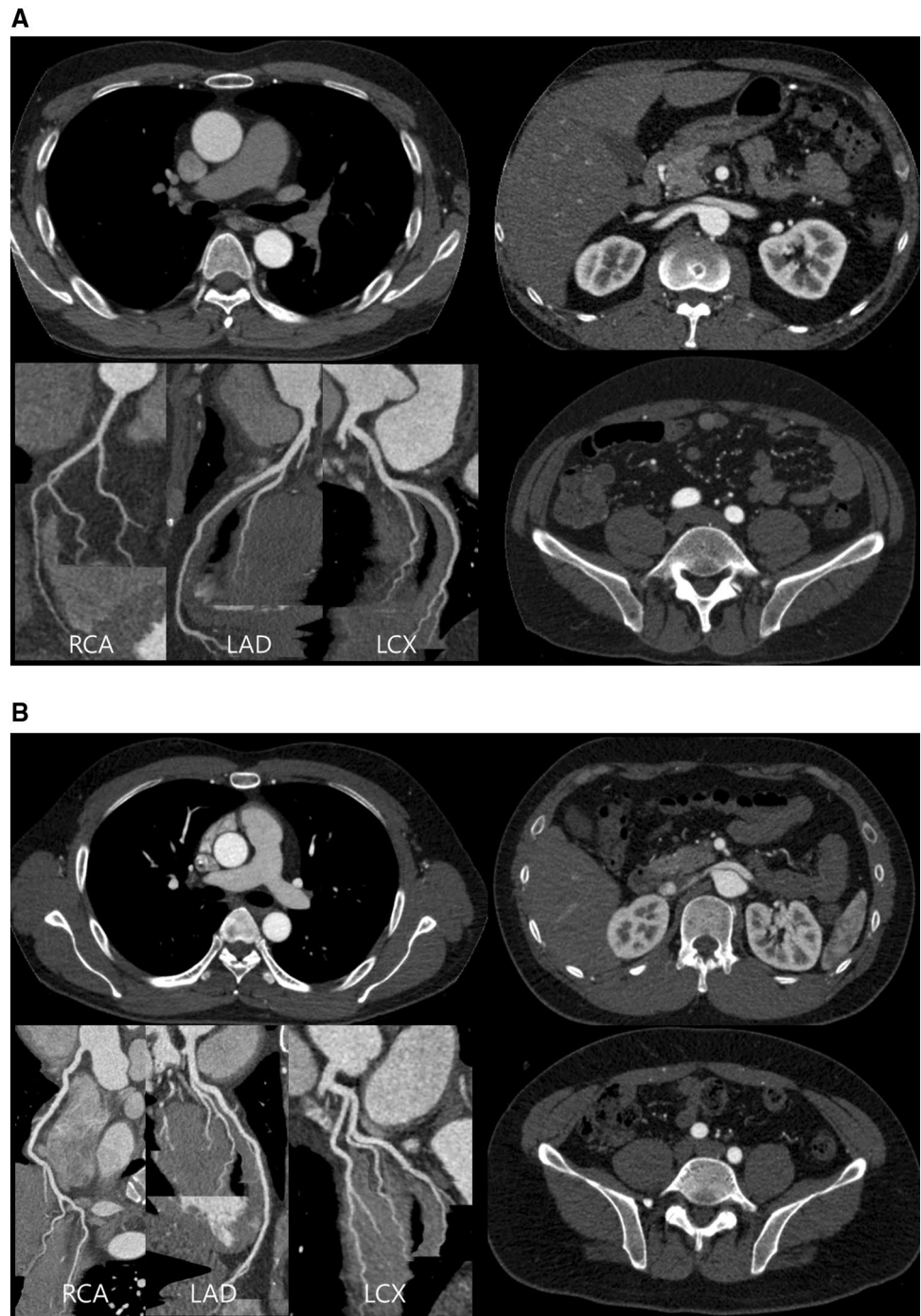
BSA body surface area, VFH volume following helical, VHP variable helical pitch

Table 2 Overall quantitative image quality measurements

	VHP	VFH	P value
Cardiac			
Vascular attenuation (HU)	560.2 ± 123.4	586.1 ± 107.3	0.386
Vessel noise (HU)	27.7 ± 9.1	28.1 ± 8.2	0.938
Image noise (HU)	30.3 ± 8.9	32.4 ± 9.0	0.266
SNR	20.1 ± 6.8	20.3 ± 10.8	0.517
CNR	24.3 ± 7.9	24.5 ± 13.2	0.439
Aortic (thoracic)			
Vascular attenuation (HU)	605.9 ± 140.2	469.2 ± 133.6	< 0.001
Vessel noise (HU)	18.2 ± 4.9	19.9 ± 4.4	0.104
Image noise (HU)	16.8 ± 6.1	18.1 ± 6.1	0.190
SNR	40.6 ± 19.5	28.4 ± 12.0	< 0.001
CNR	37.3 ± 18.5	24.8 ± 11.4	< 0.001
Aortic (abdominal)			
Vascular attenuation (HU)	498.8 ± 132.0	512.1 ± 144.5	0.662
Vessel noise (HU)	18.9 ± 4.3	20.1 ± 4.6	0.212
Image noise (HU)	20.2 ± 4.4	19.8 ± 3.8	0.601
SNR	25.6 ± 8.8	26.6 ± 8.7	0.586
CNR	22.6 ± 8.4	23.7 ± 8.6	0.519
Iliofemoral			
Vascular attenuation (HU)	497.8 ± 117.5	539.6 ± 137.7	0.143
Vessel noise (HU)	21.2 ± 4.5	21.4 ± 5.4	0.955
Image noise (HU)	21.3 ± 4.8	21.1 ± 6.6	0.774
SNR	24.4 ± 8.0	27.9 ± 11.5	0.230
CNR	22.1 ± 7.4	25.3 ± 10.9	0.233

CNR contrast to noise ratio, HU Hounsfield unit, VFH volume following helical, VHP variable helical pitch, SNR signal to noise ratio

Fig. 4 a A 45-year-old male patient referred for coronary aorta CT angiography using the VFH protocol due to chest discomfort. **b** A 36-year-old male patient referred for coronary aorta CT angiography using the VHP protocol due to chest tightness. The CT scan capture images of these two patients arranged in clockwise order are at the ascending and descending thoracic aorta (at the level of the pulmonary artery bifurcation), abdominal aorta (at each level of renal artery ostium), both common iliac arteries and coronary arteries (curved planar reformation images)



vs. 605.9 ± 140.2 HU), CNRa (24.8 ± 11.4 vs. 37.3 ± 18.5), and SNRa (28.4 ± 12.0 vs. 40.6 ± 19.5 ml) were significantly lower in VFH compared with VHP ($P < 0.001$, Table 2, and Fig. 4).

Qualitative image quality

Subjective image quality (IQ) of vascular attenuation and image artifact was assessed in two protocols (Table 3).

In assessment of the thoracic aorta, IQ scores of artifacts (4.0 ± 0.5 vs. 4.4 ± 0.6) and attenuation (4.3 ± 0.6 vs. 4.9 ± 0.3) were significantly lower in the VFH protocol compared with VHP ($P < 0.001$, Fig. 5). However, all scores obtained from the two protocols showed diagnostic image quality (grade 3–5). There were no significant differences in artifact and attenuation between the two protocols for the cardiac, abdominal aorta, and iliofemoral arteries.

Table 3 Subjective image quality measurements

	VHP	VFH	P value
Cardiac			
Artifact	4.0±0.9	4.2±0.6	0.488
Attenuation	4.4±0.7	4.5±0.6	0.469
Aortic (thoracic)			
Artifact	4.4±0.6	4.0±0.5	<.001
Attenuation	4.9±0.3	4.3±0.6	<.001
Aortic (abdominal)			
Artifact	5.0±0.0	5.0±0.2	0.362
Attenuation	4.7±0.5	4.7±0.5	0.856
Iliofemoral			
Artifact	5.0±0.0	5.0±0.1	0.528
Attenuation	4.6±0.6	4.7±0.6	0.118

VFH volume following helical scan, VHP variable helical pitch

P value was assessed by Wilcoxon rank sum test

Interobserver agreement for subjective image quality

Interobserver agreement was good or excellent for the grading attenuation and artifacts in the assessment of coronary, aorta, and iliac arteries (0.839 [95% CI: 0.805-0.867] and 0.788 [95% CI: 0.743-0.825]).

Radiation dose

The mean effective radiation dose was 706.7 ± 163.7 mGy·cm (9.9 ± 2.3 mSv) for VHP and 443.8 ± 115.8 mGy·cm (6.2 ± 1.6 mSv) for VFH. The radiation dose in the VFH was 27.2% lower than that of the VHP ($P < 0.001$).

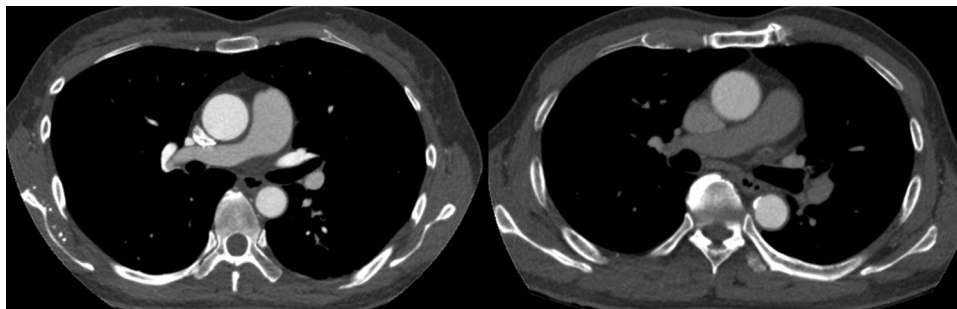


Fig. 5 The left image is acquired from a 46-year-old man using the VHP protocol, and the right image is obtained from a 73-year-old man using the VFH protocol. In the left panel, the IQ levels of the vascular attenuation and the image artifact were measured at all 5 points. On the right panel, the vascular attenuation and the image arti-

Discussion

The main finding of our study is that the image quality of VFH is comparable to that of VHP except for the thoracic aorta. The quantitative image quality scores such as vessel attenuation, SNRa, and CNRa at the thoracic aorta were significantly lower in VFH compared to VHP. However, all subjective scores obtained from the two protocols showed diagnostic image quality.

In addition, the radiation dose was significantly lower in VFH than in VHP. Various protocols have been developed to take advantage of the utility of the CT protocol for simultaneous scanning of the coronary artery and aorta. With the recent development of next-generation WDCT, VHP scan using two pitch changes and VFH scan techniques have been introduced. A previous study demonstrated the feasibility of VHP scanning for TAVI [12], but the study used VHP with only one pitch change at the diaphragmatic level and did not introduce VFH scanning. In the current study, the VHP protocol was used with two changes in the pitch at the level of carina and the base of heart. This is the first feasibility study using WDCT with the two protocols of VHP scan using two pitch changes and VFH scan.

In our study, vessel attenuation at the thoracic aorta was significantly lower in VFH (469.2 ± 133.6 HU) compared with VHP (605.9 ± 140.2 HU). This result may be due to the different sequences of scanning with the two protocols. The VHP protocol simultaneously scans the thoracic aorta and the heart, but the VFH protocol scans the heart first and then moves the CT table to the upper chest and scans sequentially. Because the contrast agent may wash out during the CT table movement from the heart to the upper chest, the measurement of vessel attenuation at the thoracic aorta may have been low. Another possibility is the difference in contrast volume between the VFH and VHP protocols (61.0 ± 7.5 vs. 72.9 ± 5.1 ml, $P < 0.001$).

fact measured were measured at all 4 points. Although, the IQ levels of vascular attenuation and image artifact measured in VFH protocol were lower than those in the VHP protocol, all scores obtained from the two protocols showed diagnostic image quality (grade 4–5)

However, in the previous study, the vessel attenuation of the thoracic aorta level was 366.78 ± 19.55 HU. and Yu Li et al. demonstrated the feasibility of using a prospective ECG-gated wide-volume protocol in CT angiography of the whole aorta and coronary arteries [15]. Considering the results of the previous study, our results for vessel attenuation of the thoracic aorta obtained from the VFH protocol are appropriate for diagnosis.

In addition, the artifact score of the thoracic aorta was lower in the VFH protocol compared with that in the VHP protocol. The VHP protocol covers proximal ascending and distal descending thoracic aorta using ECG-gated mode, but the VFH scans the thoracic aorta with non-gated data acquisition. The benefit of ECG-gated synchronization was most pronounced in the proximal ascending aorta and was less so at the aortic arch and proximal descending aorta [16]. However, subjective image quality (IQ) assessment demonstrated that the scores from the two protocols showed diagnostic image quality (grade 3–5).

The most important issue in CT scans is to reduce the radiation dose, which is particularly important for patients who will undergo repeated CT examinations. In the current study, the radiation dose with VFH was 27.2% lower than that with VHP ($p < 0.001$). Compared with the radiation dose reported in previous CT studies using VHP with one pitch change (1281.6 ± 195.7 mGy cm) [12], in our study, the radiation dose was lower in both protocols (706.7 ± 163.7 mGy·cm for VHP, 443.8 ± 115.8 mGy for VFH).

There were several limitations to our study. First, we used a qualitative scoring system that might have been influenced by subjective bias. But, the ICC values of the qualitative scoring revealed good or excellent inter-observer agreement. Second, the results of CCTA findings were not compared with those of invasive coronary angiography as the reference standard. Therefore, the diagnostic performance of CCTA for the coronary disease was not assessed. Third, this study does not represent a head to head comparison, because only two patients underwent repeated scanning for the evaluation of post-op complication. The other patients did not require repeated CT exam during the period of patients' enrollment. However, as shown in Table 1, there was no significant difference between the two groups. Fourth, our study was conducted as a single institution, and the number of patients enrolled was relatively small.

In conclusion, WDCT with single contrast injection allows simultaneous assessment of both coronary and aorta. The VFH protocol can reduce radiation dose and preserve image quality compared with the VHP protocol.

Compliance with ethical standards

Conflict of interest: The authors declare that they have no conflict of interest.

References

1. Malyshev M, Safuanov A, Borovikov D et al (2008) Simultaneous multi-vessel coronary artery bypass grafting, ischemic mitral regurgitation repair and descending aortic aneurysm replacement: analysis of technical points. *Interact Cardiovasc Thorac Surg* 7(2):315–317
2. Furutachi A, Rikitake K, Ikeda K et al (2014) Simultaneous thoraco-abdominal aortic aneurysm repair and coronary artery bypass grafting through median sternotomy. *Ann Thorac Surg* 98(3):1081–1083
3. Eren E, Toker ME, Tuncer A et al (2007) Surgical management of coronary malperfusion due to type a aortic dissection. *J Card Surg* 22(1):2–6
4. Neri E, Toscano T, Papalia U et al (2001) Proximal aortic dissection with coronary malperfusion: presentation, management, and outcome. *J Thorac Cardiovasc Surg* 121(3):552–560
5. Kawahito K, Adachi H, Murata S et al. (2003) Coronary malperfusion due to type A aortic dissection: mechanism and surgical management. *Ann Thorac Surg* 76(5):1471–1476; **discussion 1476**
6. Kang EJ, Kim SM, Choe YH et al (2014) Takayasu arteritis: assessment of coronary arterial abnormalities with 128-section dual-source CT angiography of the coronary arteries and aorta. *Radiology* 270(1):74–81
7. Soto ME, Melendez-Ramirez G, Kimura-Hayama E et al (2011) Coronary CT angiography in Takayasu arteritis. *JACC Cardiovasc Imaging* 4(9):958–966
8. Leipsic J, Gurvitch R, Labounty TM et al (2011) Multidetector computed tomography in transcatheter aortic valve implantation. *JACC Cardiovasc Imaging* 4(4):416–429
9. Schoenhagen P, Kapadia SR, Halliburton SS et al (2011) Computed tomography evaluation for transcatheter aortic valve implantation (TAVI): imaging of the aortic root and iliac arteries. *J Cardiovasc Comput Tomogr* 5(5):293–300
10. Salgado RA, Leipsic JA, Shivalkar B et al (2014) Preprocedural CT evaluation of transcatheter aortic valve replacement: what the radiologist needs to know. *Radiographics* 34(6):1491–1514
11. Lewis MA, Pascoal A, Keevil SF et al (2016) Selecting a CT scanner for cardiac imaging: the heart of the matter. *Br J Radiol* 89(1065):20160376
12. Matsumoto S, Yamada Y, Hashimoto M et al (2017) CT imaging before transcatheter aortic valve implantation (TAVI) using variable helical pitch scanning and its diagnostic performance for coronary artery disease. *Eur Radiol* 27(5):1963–1970
13. Felmly LM, De Cecco CN, Schoepf UJ et al (2017) Low contrast medium-volume third-generation dual-source computed tomography angiography for transcatheter aortic valve replacement planning. *Eur Radiol* 27(5):1944–1953
14. Shrimpton PC, Hillier MC, Lewis MA et al (2006) National survey of doses from CT in the UK: 2003. *Br J Radiol* 79(948):968–980
15. Li Y, Fan Z, Xu L et al (2012) Prospective ECG-gated 320-row CT angiography of the whole aorta and coronary arteries. *Eur Radiol* 22(11):2432–2440
16. Hayter RG, Rhea JT, Small A et al (2006) Suspected aortic dissection and other aortic disorders: multi-detector row CT in 373 cases in the emergency setting. *Radiology* 238(3):841–852

Publisher's Note Note Springer Nature remains neutral with regard to jurisdictional claims in published maps and institutional affiliations.